Nanotechnology Perceptions
ISSN 1660-6795
www.nano-ntp.com

Physiochemical Properties of Capping Agent Mediated $NiFe_2O_4$ Nanoparticles AndTheir Antibacterial Applications

P.Priyadharshini[1], G.Mahalakshmi[1*]

[1]Department of Physics, Government arts college-Karur-639005 (Affiliated to Bharathidasan University), Tamilnadu
E.mail: arunamaha@gmail.com, dharshini0694@gmail.com
*Corresponding Author : G.Mahalakshmi**

In this study, $NiFe_2O_4$ magnetic nanoparticles have been produced using a simple precipitation technique with some capping agents ,and the effect of capping agents on structural, optical and antibacterial properties was investigated in detail. The average crystallite size obtained by the Scherrer technique ranges from 20 to 54 nm. PL spectroscopy reveals the optical properties of nickel ferrite nanoparticles. The elemental composition and chemical binding has been investigated by x-ray photoelectron spectroscopy. The antibacterial activity of capping agent-assisted nickel ferrite nanoparticles were examined against two gram-positive bacteria, S.aureus and E.faecilis, as well as two gram-negative bacteria, E.coli and P.aeroginosa

Keywords: Nickel ferrite, Capping agent, Antibacterial activities, Photoluminescence.

Introduction

The metallic components such as, Ba, Mn, Ni, Cu, Co and Zn are mixed and fired with Fe_2O_3 which produces ceramic materials known as ferrites. Ferrites are both electrical insulators and ferromagnetic so that they can be magnetized easily. According to their magnetic properties, ferrites are categorized into two types: hard ferrites and soft ferrites. Soft ferrites have a low coercivity value, making them quickly magnetized and demagnetized, hard ferrites possess a high coercivity value, which makes them hard to magnetize and demagnetize. Based on the crystal structure and cation distribution, they are considered as (i) spinel ferrites and (ii) inverse spinel ferrites with the common chemical formula MFe_2O_4, where M is a divalent metal cation [1]. The spinel ferrite is a face-centered cubic (fcc) lattice composed of oxygen ions and the space group fd3m. It has 32 oxygen atoms in an fcc lattice, with metal ions split into 8 tetrahedral A sites and 16 octahedral B sites [2, 3]. Ferrite nanomaterials are gaining attention in a variety of emerging fields, including high- density storage devices, microwave devices, recording tapes, telecommunication applications, and different life science applications, such as drug delivery to certain areas of the body, magnetic cell separation, and magnetic resonance

imaging. [4,5]. $NiFe_2O_4$ nanoparticles have drawn continual attention among various types of ferrites due to their unique structural, optical, magnetic, thermal catalytic, and chemical abilities throughout recent decades. $NiFe_2O_4$ is well-known as a ferromagnetic material with high intrinsic resistivity, low coercivity, low dielectric and magnetic losses, a stable chemical composition and mechanical strength, and high curie temperatures to maintain its magnetic properties [6]. $NiFe_2O_4$ is essentially an inverse spinel, with half of the iron ions preferentially occupying the tetrahedral A sites while the other half being surrounded by the octahedral B sites [7,8].

A clear literature survey reveals that many researchers are studying the effect of surfactants assisted ferrite nanoparticles like CTAB, Oleic acid, PVA, PEG, PVP and SDS, etc. on the structural optical and magnetic properties. Effects of surfactants assisted $NiFe_2O_4$ nanoparticles were done by M.M.L.Sonia et.al using PVB/EDTA/CTAB as the surfactants through sol-gel synthesis method and studied their structural magnetic and dielectric properties. They observed that the use of various surfactants in the sample preparation modifies the size of $NiFe_2O_4$, which drastically affects its magnetic parameter [9]. P.Sivakumar et.al prepared nickel ferrite magnetic nanoparticles by using a polyvinyl alcohol (PVA) as a surfactant through the sol-gel auto combustion method. They were reported that the microstructural analysis described that nickel ferrite nanoparticles had spherical, narrow size and uniform distribution [10]. A.Baykal et.al have studied the CTAB assisted hydrothermal synthesis and magnetic characterization of $Ni_xCo_{1-x}Fe_2O_4$ nanoparticles (x=0.0, 0.6, 1.0). They established that the particles revealed very high phase purity and crystallinity, making them appropriate for magnetic recording applications [11]. S.Asiri et al. showed that the improvement of the maximum magnetization and the magnetic moment of the $NiFe_2O_4$ nanoparticles were increased as the temperature increased [7]. P.Iranmanesh et.al did their investigation on superior magnetic properties of Ni Ferrite nanoparticles synthesized by capping agent free one-step co-precipitation route at different pH values. They discovered that optical examination demonstrated that $NiFe_2O_4$ nanoparticles had indirect band gap materials, and their band gap values rise with the level of pH, permitting the formation of larger particles with fewer surface effects [12]. Several chemical techniques have been established to synthesize nickel ferrite nanoparticles, including hydrothermal approach [13] Sol-gel [14], thermal decomposition approach [15], Mechanochemical approach [16], Ball milling approach [17], coprecipitation approach [18], and Solid state reaction approach [19]. Among, the various synthesis techniques, co-precipitation method received a lot of attention in the production of nickel ferrite nanoparticles due to several advantages, such as economical, simple, easy reliability, and particle shape and size control, to obtain huge quantities of $NiFe_2O_4$ nanoparticles [20] and there is no need of microwave heat or extra mechanical treatments [18]. Besides from that, the precipitation approach produces smaller nanoparticles than the sol-gel and hydrothermal methods [21]. Because of such advantages, the co-precipitation approach was chosen for the preparation of surfactant-assisted $NiFe_2O_4$ nanoparticles, and the structural, optical, morphological, and magnetic properties were thoroughly examined. In this work, we examine the synthesis of nickel-ferrite nanoparticles by means of surfactant assisted co-precipitation method. Characterization by various analytical techniques of synthesized nanoparticles, such as, XRD, Raman, TEM, XPS and so on summed up here.

Experimental Procedure

Methodology

Analytic grade nickel Chloride hexahydrate ($NiCl_2.6H_2O$), Iron (III) Chloride ($FeCl_3.4H_2O$), Sodium hydroxide (NaOH) were used as starting materials. Oleic acid CTAB, PVA and PEG with a molecular weight of 800 g/mol were utilized as capping agents. Each of the compounds had been used in the synthesis procedure without any further purification.

Synthesis of capping agent assisted $NiFe_2O_4$ nanoparticles

Fine $NiFe_2O_4$ nanoparticles were produced by using co-precipitation method. Nickel chloride, iron chloride, and NaOH aqueous solutions were prepared separately by dissolving each chemical in water that was double-distilled. In order to produce $NiFe_2O_4$, 1M $NiCl_2.6H_2O$ and $FeCl_3.4H_2O$ were dissolved in 50ml of water that was double-distilled at 80°C for a 10-minute period while being constantly stirred. After combining the aforementioned solutions, 100 mL of 3M solution of sodium hydroxide was added drop-wise while rotating continuously until the pH level reached 14. A certain amount of Oleic acid, CTAB, PEG and PVA was added to the aforesaid solution as a capping agent. The homogeneous solution was stirred for 3hours at 80°C. The intermediate hydroxides transformed into spinal ferrite within this 3h duration. After allowing the finished solution to reach room temperature and then it precipitated for three days. The resulting material was then washed repeatedly with ethanol and double-distilled water until the pH of the solution was decreased to 7, at after which it was filtered. The moist sedimentation was dried and processed into a fine powder. At last the synthesized nickel ferrite nanopowder have been annealed at 800°C for 4 hours to eliminate water molecules and undesirable contaminants in order to obtain a high crystallinity in the sample.

Characterization techniques of $NiFe_2O_4$

The fabricated powder sample performed structural analysis using a PAN analytical X'pert Pro X-ray diffractometer. Emission properties of the synthesized samples were studied by PL spectrometer (Kimono, SPEC-14031k, Japan) at room temperature in the wavelength range from 350-650 nm with He-Cd laser line of 325 nm. With a 300kV accelerating voltage and a high-resolution pole piece, a transmission electron microscope was employed to examine the microstructure of the prepared sample. We have investigated the antibacterial activities of capping agent-assisted nickel ferrite nanoparticles against gram-positive (S. aureus and E. faecilis) and gram-negative (E. coli and P. aeruginosa) bacterial pathogens using an agar well diffusion technique.

Results and Discussion

Structural Analysis

The XRD spectra of capping agents (Oleic acid, CTAB, PVA and PEG) assisted and pure Nickel ferrite nanoparticles are shown in Figure 1. Crystal structure, phase purity, and size of the produced materials are evaluated using XRD. All the synthesized samples were examined using powder X-software and then the XRD peaks compared to standard number 44-1485. The

XRD data revealed the observation of a single phase cubic spinal shape with peaks at 2θ =18.3686°, 30.3052°, 35.6882°, 37.3716°, 43.3859°, 53.8054°, 57.3248°, 62.9727°, 63.1033° and 74.6165° corresponds to the crystal planes (111), (220), (311), (222), (400), (422), (511) and (440) respectively [21]. The synthesized samples contained no diffraction peaks of other impurities such as α-Fe_2O_3 and NiO are observed within the limitations of X-ray detection [22]. The broadness of the observed peaks indicated the nanoscale range of crystallites, as well as the number of peaks confirmed the polycrystalline structure of the materials [23].

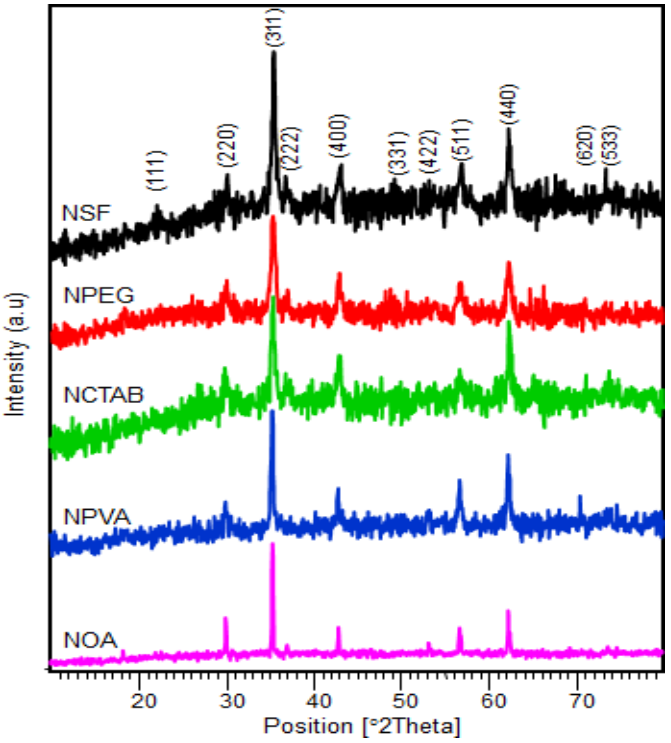

Figure 1. XRD patterns of $NiFe_2O_4$ samples using different capping agents.

The prominent The XRD peaks of the $NiFe_2O_4$ sample coated with oleic acid suggest that the oleic acid strengthened the crystallinity of the $NiFe_2O_4$ nanoparticles. This shows that the nucleation rate is higher in the NSF, NPEG, NCTAB, and NPVA samples than the growth rate, indicating that the surfactant has a significant impact on the nucleation and growth rates, which in turn determines the crystallite size [24]. From the sharpest peak of (311) the size of crystallite (D) of the samples was calculated using the Debye-Scherrer formula [25]

$$D = \frac{0.9\lambda}{\beta\cos\theta} \text{ nm}$$

where λ is denoted by radiation wavelength, β represents the full-width at half maximum whereas θ represents angle of diffraction. The calculated crystalline sizes of the developed nickel ferrite nanoparticles are 54 nm, 27 nm, 16.2 nm, 32.4 nm, and 32.4 nm, respectively. Likewise A.Baykal et.al have obtained the crystalline size for nickel ferrite nanoparticles in the range 15 nm – 55 nm [26]. The lattice parameter 'a' was established using the formula

$$a=d\sqrt{h^2 + k^2 + l^2}$$

where (hkl) refers to the miller indices and d indicates the spacing between two planes [5]. The lattice constant was determined to the synthesized nickel ferrite is 8.3442Å, 8.3367 Å, 8.3622 Å, 8.3542 Å, and 8.3416 Å respectively. The calculated lattice constants are slightly bigger compared to those of bulk $NiFe_2O_4$ [8.339 Å, JCPDS card No: 44-1485]. To obtain the lattice constant a' accurately for each sample, the Nelson-Riley function F(θ) was used;

$$F(\theta) = \frac{1}{2}\left[\frac{\cos^2\theta}{\sin\theta} + \frac{\cos^2\theta}{\theta}\right]$$

Using the least square fit method, the lattice constant 'a' of all the peaks for every sample was plotted opposed to the error function F(θ). The lattice constant of the composition is determined by the point where the least square fits a straight line and cuts the y-axis, where F(θ) = 0. The lattice constant (a') for the NSF, NPEG, NCTAB, NPVA, and NOA samples were determined to be 8.3287, 8.3383, 8.3305, 8.3512, and 8.3415Å, respectively. Figure 2 displays the determination of the lattice constant using the Nelson-Riley function F(θ).

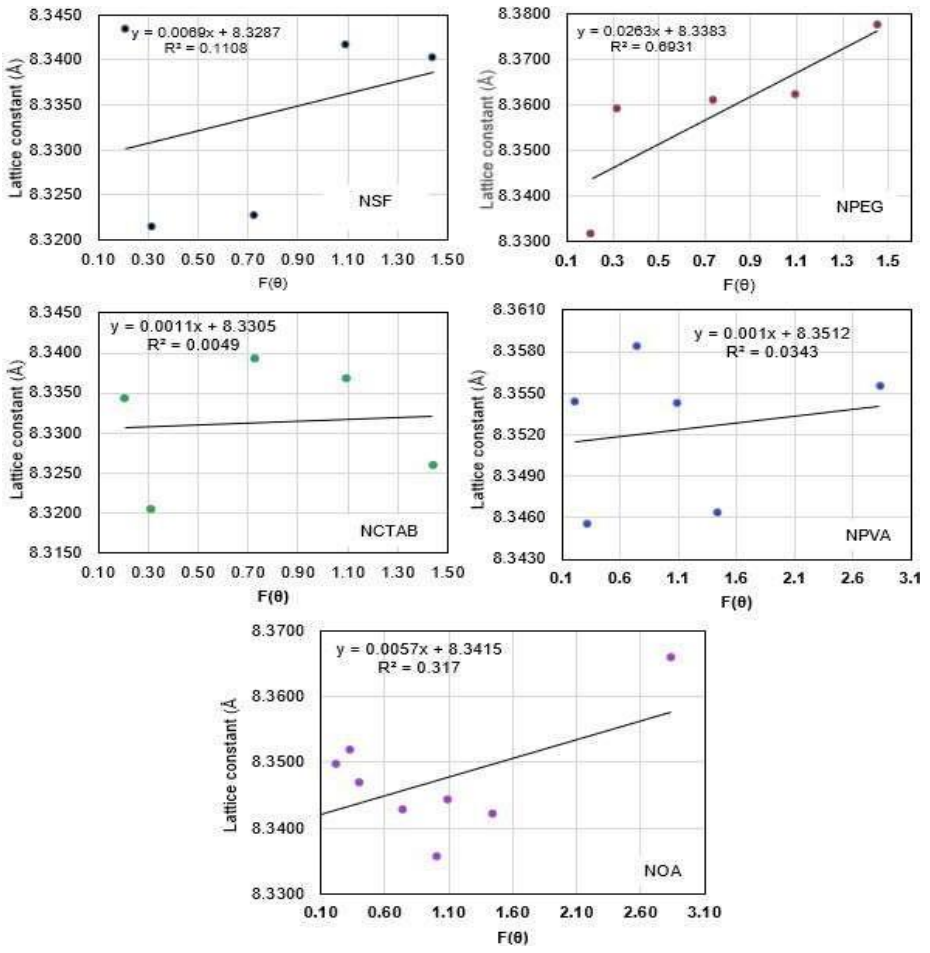

Figure 2. Nelson-Riley function of $NiFe_2O_4$ magnetic nanoparticles using different capping agent

PL Spectroscopy

PL spectra of the described materials are shown in Figure 3. Peaks of intrinsic emission are observed in the PL spectra between 360 and 595 nm. It is notable that the position of the emission peak did not change, but the intensities changed. Near band edge emissions, which result from the recombination during the free exciton moving from the localized level below the conduction band to the valence band, are responsible for the peak UV emission at 360 and 376 nm [27]. The violet emissions detected between 408 and 438 nm indicate that the conduction band edge may be the beginning point for the violet emission.

These results attributed to the first conclusion that violet emission may be efficiently stimulated at an excitation wavelength within the band gap of $NiFe_2O_4$ nanoparticles. The emission peaks at 492, 506, and 542 nm, and 595 nm, correlate to green emission, which is

mostly caused by surface defects or oxygen vacancies. Aside from providing evidence directly for the origin of green emission, it is anticipated that the optical properties of $NiFe_2O_4$ nanocrystallites will be tunable by crystal surface control. The present study would surely enhance the usability of surface architecture-controlled $NiFe_2O_4$ nanoparticles in optoelectronic devices.

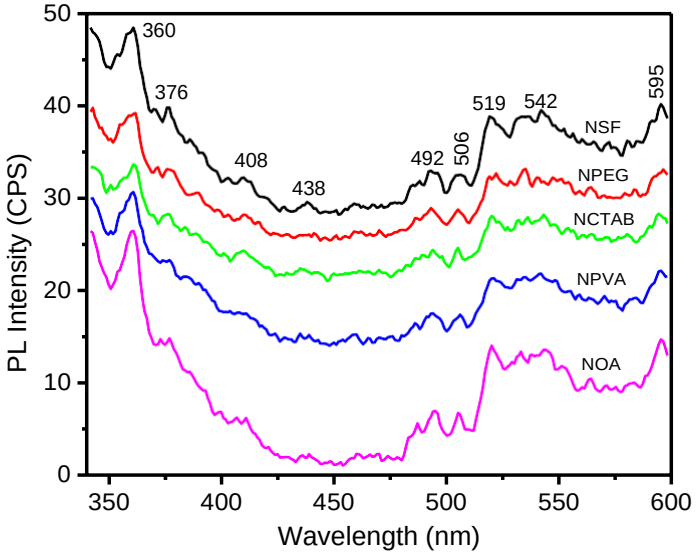

Figure 3. Photoluminescence spectrum of $NiFeO_4$ nanoparticles

Furthermore, the PL spectrum has been assigned to charge channeling between Fe^{3+} and Ni^{2+} sites enclosed by O^{2-} ions [28]. Similar results were previously reported by A.Nadumane et.al [29] and they found an emission peak in the visible region between 420 and 630 nm. Chand et al. [30] observed UV emission (389 nm) and blue emissions (471 nm) in $CoFe_2O_4$, $NiFe_2O_4$, and $ZnFe_2O_4$ nano-ferrite particles.

TEM and EDAX analysis

Figure 4 shows the findings of morphological analysis of synthesized nickel ferrite nanoparticles using TEM to elucidate their structural features. Image J software was used to compute particle size and interplanar spacing, as well as to index the SAED pattern rings. Figure 4 shows a TEM picture of the oleic acid (NOA)-assisted $NiFe_2O_4$ sample obtained from a single spherical nanoparticle. The particles are spherical and regular in shape. The micrograph shows nanoparticles with tiny grains from 35 to 65 nm without

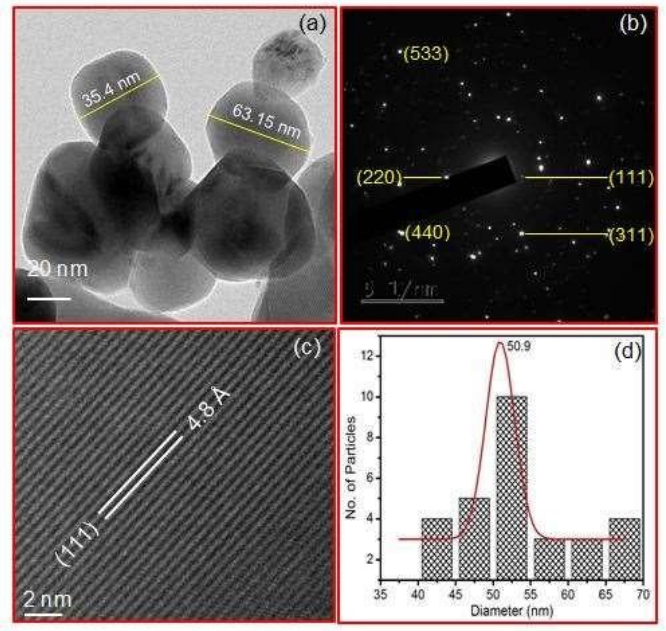

Figure 4. TEM images of Oleic acid sample. Here (a) TEM image, (b) SAED pattern, (c) Frindge width pattern (d) Particle size distribution curve

any pores, demonstrating that the oleic acid is an excellent capping agent to achieve a spherical shaped nanoparticle [31]. The selected area diffraction pattern exhibits consecutive circles around a sharp point, indicating that the produced materials are polycrystalline. Furthermore, It is well-indexed to (220), (311), (440), and (511) Miller's planes of the cubic face-centered spinel structure, which is accordance with XRD results [32]. The SAED pattern has d-spacing of 4.8Å, 2.5 Å, and 2.3 Å, corresponding to the (111), (311), and (222) planes of capping agent-assisted $NiFe_2O_4$ [33]. Thus, the TEM analysis demonstrates that the capping substance plays a vital role in establishing the size of the magnetic nanoparticle.

The elemental composition of $NiFe_2O_4$ nanoparticles was investigated using energy dispersive x-ray spectrum analysis, and the findings are shown in Table 1. An EDAX spectrum was obtained for all the samples, however the typical EDAX spectrum of the NOA sample individually has been shown in Figure 5. The spectrum indicates the presence of Ni^{2+}, Fe^{3+}, and O^{2+} in the synthesized $NiFe_2O_4$ sample. There is no other impurity elements detected, which indicates the high quality of the synthesized sample.

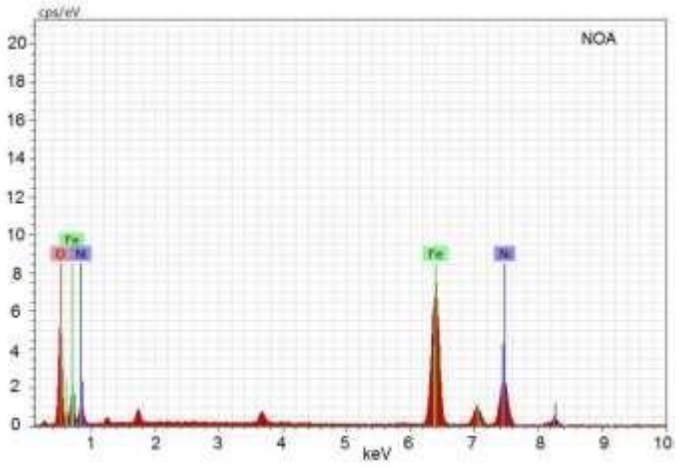

Figure 5. EDAX spectrum of OA coated $NiFe_2O_4$ samples

Table 1. EDAX data of capping agents assisted $NiFe_2O_4$ nanoparticles

Chemical composition	Elements in (wt%)			Elements in (at%)			Total (%)
	Ni	Fe	O	Ni	Fe	O	
NOA	10.14	20.24	69.52	3.54	7.43	89.03	100

Analysis of Surface composition and oxidation state of $NiFe_2O_4$ by XPS

The findings of an XPS analysis to identify the surface composition and oxidation state of the as-synthesized $NiFe_2O_4$ products are displayed in Figure 6(a-d). The survey spectrum (Figure. 6a) clearly shows the distinct peaks for the elements Ni, Fe, O, and Cl with no extraneous impurity peaks. Two spin–orbit doublets and two shake-up satellite peaks comprise the Ni 2p core-level spectrum (Figure. 6b). First and foremost two strong peaks at binding energy levels of 855.6 and 873.8 eV revealed dual spin-orbit peaks of Ni $2p_{3/2}$ and Ni $2p_{1/2}$, confirming the existence of Ni^{2+} as well as Ni^{3+} [34]. Furthermore, two satellite peaks roughly at 862.1 and 878.9 eV were widely regarded as representative Ni shake-up type peaks, and their existence enabled researchers to efficiently investigate the chemical state [35]. The Fe2p detailed spectrum (Figure 6c) reveals two distinct peaks at 710.3 and 723.8 eV, which correspond with Fe $2p_{3/2}$ and then Fe $2p_{1/2}$ spin-orbit peaks, respectively, and they identify the Fe^{3+} state of oxidation in the $NiFe_2O_4$ products. In the high-resolution spectra, two oxygen peaks were detected in the O 1s region at 529.98 and 531.38 eV, respectively. It was established that the first peak, at 529.98 eV, represented a normal M-O bond. However, the second peak, at 531.38 eV, may be attributed to defect sites such as hydroxyls, carboxyls, or species inherent in the spinel structure's surface [36]. The high-resolution spectra of C 1s reveal three valence bonds (C=O, C-O, and C-

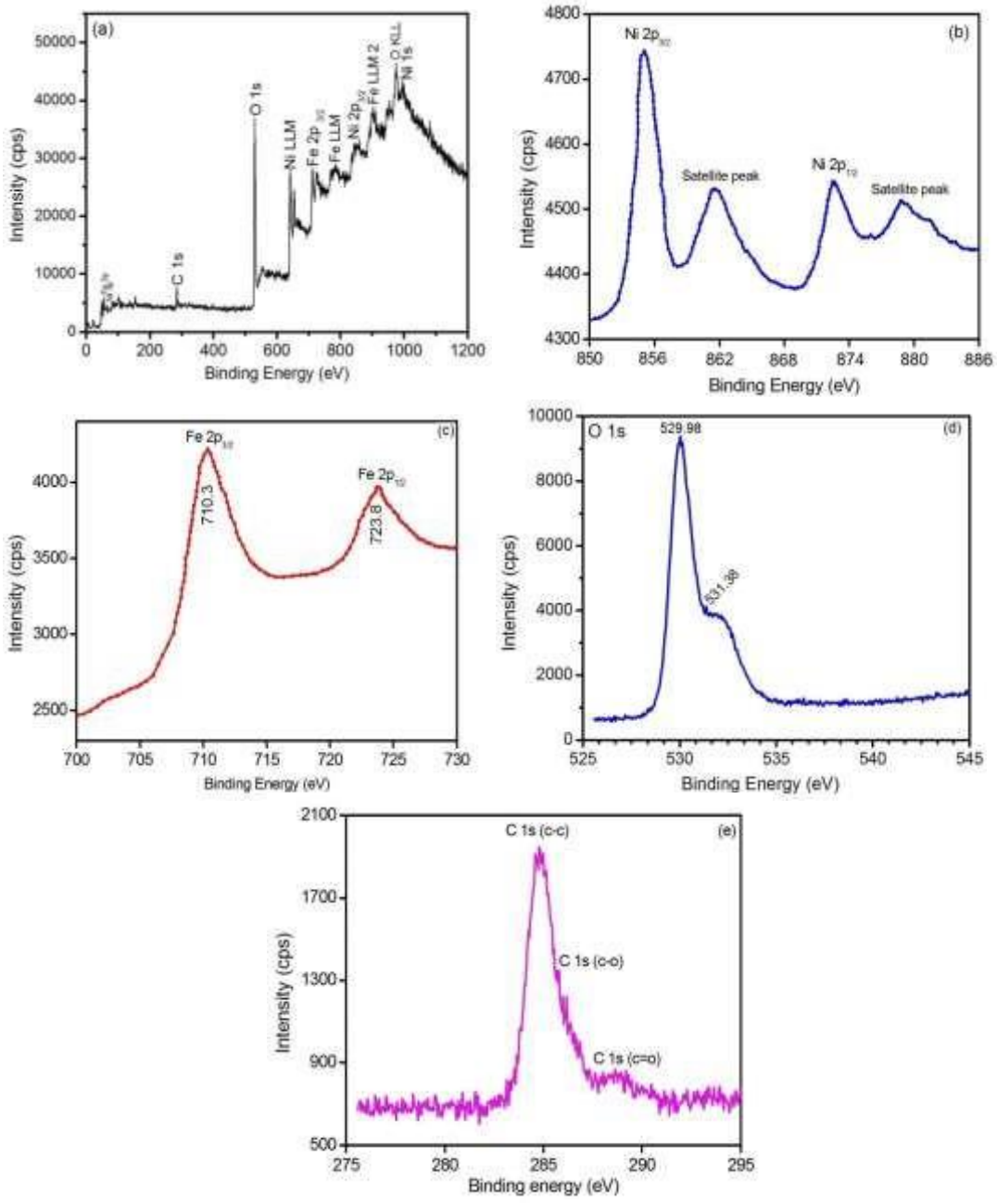

Figure 6. XPS spectra of oleic acid assisted $NiFe_2O_4$magnetic nanoparticle (a) survey spectrum; (b) Ni-2p binding energy spectrum; (c) Fe-2p binding energy spectrum, (d) O-1s binding energy spectrum, and(d) C-1s binding energy spectrum

C) with energies of 288.3 eV, 285.4 eV, and 284.5 eV, respectively [37, 38]. These bonds are related to the addition of all carbon attributions associated to at least one oxygen atom [39].

Antibacterial activities of Nickel ferrites

The following microorganisms were used to assess the antibacterial properties of nickel ferrite nanoparticles: E. Coli, Pseudomonas aeruginosa, Staphylococcus aureus, and Enterococcus faecilis. The antibacterial properties of $NiFe_2O_4$ nanoparticles were determined via agar well diffusion method. The chosen bacterium was based on a widespread infection impacting society as a result of their intake when present in polluted water or air, among other things for example the presence of E.coli causes nausea, a very pathogenic microorganism like Pseudomonas aeruginosa causes diarrhea both children and adults can suffer from whooping cough.

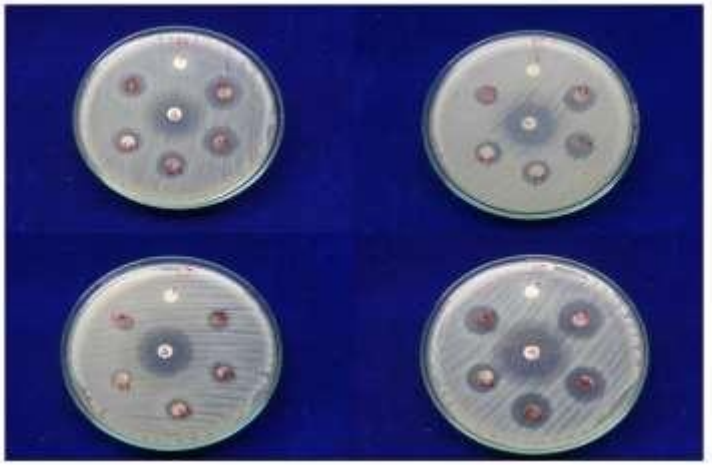

Figure 7. Antibacterial activities of synthesized $NiFe_2O_4$ nanoparticles

Table 2. Antibacterial Assay of $NiFe_2O_4$ nanoparticles

S. No.	**Bacteria**	**Zone of inhibition (mm in diameter)**						
		C	S* (Amoxycillin)	SF	PEG	PVA	CTAB	Oleic acid
1	**E. coli**	-	21	14	13	14	17	18
2	**E. faecalis**	-	22	10	12	13	13	15
3	**P. aeruginosa**	-	23	10	10	10	10	10
4	**S. aureus**	-	27	14	14	17	18	20

Meantime, the effect of Staphylococcus aureus causes complications in wounds. The outcomes of antibacterial activities are shown in Figure. 6 (a-d) and the Zone of inhibition is shown in the table 2. Capping agent assisted $NiFe_2O_4$ show the antibacterial activity on gram-negative bacterium E.coli and Pseudomonas aeruginosa. E.coli has increasing inhibition zone in 14 to 18mm and Pseudomonas aeruginosa has 10mm zone of inhibition in prepared nanoparticles. The effect of capping agent assisted $NiFe_2O_4$ on gram-positive bacterium S.aureus and Enterococcus faecalis, there was gradually increased in inhibition zone from 14 to 20 mm and 10 to 15 mm respectively. This antibacterial activity is a suitable source of disinfectant in a contaminated water body, with efficient qualities which improves microbe inhibition on S. aureus and Pseudomonas aeruginosa, as developed by nickel ferrites nanoparticles [40].

Conclusion

In conclusion, we have effectively prepared nickel ferrite nanoparticles using the chemical precipitation technique without and with several surfactants such as PEG, PVA, CTAB, and OA. The structural, optical, and emission characteristics of synthesized materials were investigated. The XRD study confirms that the synthesized samples contain a cubic spinel structure. Surfactants have varying average cryst0allite sizes and lattice constants, ranging from 20 to 54 nm and 8.3376 to 8.3622Å. The UV emission of the $NiFe_2O_4$ samples was confirmed by the PL spectra. The TEM analysis indicates that $NiFe_2O_4$ nanoparticles are sensitive to surfactants. Finally, it is proven that capping agents have a crucial function in influencing particle size.

Author Contributions:
Priyadharshini - Perception, methodology, writing original draft and editing,
Mahalakshmi – supervision and submission of manuscript to journal and follow up action.
Authors have read and agreed to publish the final version of the manuscript.

Funding: This research received no external funding.

Conflicts of Interest: Authors declare no conflict of interest.

Acknowledgment
The authors are grateful to Instrumentation centre-karaikudi for providing XRD and PL characterizations, and STIC – Cochin for providing TEM facilities.

References

1. P.Monisha, P.Priyadharshini, S.S.Gomathi, K.Pushpanathan, Ferro to superparamagnetic transition: Outcome of Ni doping in polyethelene glycol capped CoFe2O4 nanoparticles, Journal of Alloys and compounds, 2020, 157447.

2. A.A.Ati, Z.Othaman, A.Samavati, Influence of Cobalt on structural and magnetic properties of nickel ferrite nanoparticles, Journal of Molecular structure, 1052, 2013 177-182

3. H.Hajihashemi, R.Kameli, H.Salamati, The effect of EDTA on the synthesis of Ni ferrite nanoparticles, Journal of super conductivity and novel magnetism, 25, 2012, 2357-2363

4. A.Ahlawat, V.G.Sathe, V.R.Reddy, A.Gupta, Mossbauer, raman and x-ray diffraction studies of superparamagntic NiFe2O4 nanoparticles prepared by sol-gel auto-combustion method, Journal of magnetism and magnetic materials, 323 (2011) 2049-2054

5. S.K.E.Islam, P.Sharma, Synthesis and characterization of nickel ferrite:Role of Sintering temperature on structural parameters, Journal of nano-and electronic physics, 6, (2014) 01008

6. M.H.Khan, I.H.Gul, M.M.Baig, H.N.Khan, Comprehensive study on structural electrical magnetic and photocatalytic degradation properties of Al3+ ions substituted nickel ferrites nanoparticles, Journal of Alloys and Compounds, 848, (2020) 155795

7. S.Asiri, M.Sertkol, H.Gungunes, Md.Amir, AA.Manikandan, I.Ercan, A.Baykal, The temperature effect on magnetic properties of NiFe2O4 nanoparticles, Journal of Journal of Inorganic and organometallic polymers and materials, 28, 2018, 1587-1597.

8. A.C.F.M.Costaa, V.J.Silvaa, D.R.Cornejob, M.R.Morellic, R.H.G.A.Kiminamic, L.Gama, Magnetic and structural properties of NiFe2O4 ferrite nanopowder doped with Zn^{2+}, Journal of Magnetism and Magnetic materials, 320, (2017) e370-e372.

9. M.M.L.Sonia, S.Anand, S.Blessi, S.Pauline, A.Manikandan, Effect of surfactants (PVB/EDTA/CTAB) assisted sol-gel synthesis structural magnetic and dielectric properties of $NiFe_2O_4$ nanoparticles, Ceramics international, 44 (2018) 22068-22079.

10. P.Sivakumar, R.Ramesh, A.Ramanand, S.Ponnusamy, C.Muthamizhchelvan synthesis and characterization of nickel ferrite magnetic nanoparticles, Materials research Bulletin, 46, (2011) 2208-2211

11. A.Baykal, N.Kasapoglu, Z.Durmus, H.Kavas, M.S.Toprak, Y.Koseoglu, CTAB assisted hydrothermal synthesis and magnetic characterization of $Ni_xCo_{1-x}Fe_2O_4$ nanoparticles (x=0.0, 0.6, 1.0) Turk J Chem, 33 (2009), 33-45.

12. P.Iranmanesh, Sk.T.Yazdi, M.Mehran, S.Saeednia, Superior Magnetic properties of Ni ferrite nanoparticles synthesized by capping agent free one step coprecipitation route at different pH values,Journal of Magnetism and Magnetic materials, 449 (2018) 172-179.

13. K.Nejati, R.Zabihi, Preparation and magnetic properties of nano size nickel ferrite particles using hydrothermal method, Chemistry Central Journal, 6:23, (2012) 1-6

14. M.M.L.Sonia, S.Anand, V.M.Vinosel, M.S.Janifer, S.Pauline, A.Manikandan, Effect of lattice strain on Structure morphology and magneto-dielectric properties of $NiGd_xFe_{2-x}O_4$ ferrite nanocrystallites synthesized by sol-gel route, Journal of Magnetism and Mangentic Materials, 466 (2018) 238-251

15. X.Lasheras, M.Insausti, I.G.D.Muro, E.Garaio, F.Plazaola, M.Moros, L.D.Matleis, J.M.De la Fueta and L.Lezama, Chemical synthesis and magnetic properties of monodisperse nickel ferrite nanoparticles for biomedical applications, The journal of physical chemistry, 2016, 120, 3492-3500.

16. Y.Shi, J.Ding, H.Yin, CoFe2O4 nanoparticles prepared by the mechanochemical method, Journal of alloys and compounds, 308, (2000) 290-295.

17. C.N.Chinnasamy, A.Narayanasamy, N.Ponpandian, R.J.Joseyphus, B.Jeyadevan, K.Tohji, K.Chattopadhyay, Grain size effect on the Neel Temperature and magnetic properties of nanocrystalline NiFe2O4 spinel, Journal of Magnetism and magnetic materials, 238 (2002) 281-287.

18. K.Maaz, S.Karim, A.Mumtaz, S.K.Hasanain, J.Liu, J.LDuan, Synthesis and magnetic characterization of nickel ferrite nanoparticles prepared by co-precipitation route, Journal of magnetism and magnetic materials, 321, (2009) 1838-1842.

19. F.L.Zabotto, A.J.Gualdi, J.A.Eiras, A.J.A.D.Oliveira, D.Garcia, Influence of the sintering temperature on the magnetic and Electric properties of NiFe2O4 ferrites, Materials Research, 15, 2012, 428-433.

20. P.Monisha, P.Priyadharshini, S.S.Gomathi, P.Mahendran, K.Pushpanathan, Influence of Mn dopant on the crystallite size optical and magnetic behavior of $CoFe_2O_4$ magnetic nanoparticles, Journal of physics and chemistry solids, 148 (2021) 109654.

21. P.Monisha, P.Priyadharshini, S.S.Gomathi, M.Mahendran K.Pushpanathan, Role of Zn dopant on superparamagnetic property of $CoFe_2O_4$ nanoparticles, 2019 Applied Physics A.

22. S.Joshi, M.Kumar, S.Chhoker, G.Srivastava, M.Jewariya, V.N.Singh, Structural magnetic dielectric and optical properties of Nickel ferrite nanoparticles synthesized by co-precipitation method, Journal of Molecular Structure, 1076, 55-62, (2014).

23. P.Priyadharshini, K.Pushpanathan, V.Kathiravan, Effect of Surfactants on the structural and magnetic properties of $NiFe_2O_4$ nanoparticles, Asian Journal of Chemistry, 34,9 (2022), 2406-2414

24. K.Lawrence, K.Pawan, N.Amarendra, K.Manoranjan, Rietvield analysis of XRD patterns of different sizes of nanocrystalline cobalt ferrite, International Nano Letters,3 (2013) 1-12

25. A.L.Patterson, the scherrer formula for X-ray particle size determination Phys.Rev 56, 978 (1939)

26. A.Baykal, N.Kasapoglu, Y.Koseoglu, M.S.Toprak, H.Bayrakdar, CTAB assisted hydrothermal synthesis of $NiFe_2O_4$ and its magnetic characterization, Journal of Alloys and Compounds, 464 (2008) 514-518

27. H.Harzali, A.Marzouki, F.Saida, A.Megriche, A.Mgaidi, Structural magnetic and optical properties of nanosized $Ni_{0.4}Cu_{0.2}Zn_{0.4}R_{0.05}Fe_{1.95}O_4$ ($R=Eu^{3+}$, Sm^{3+}, Gd^{3+}, and Pr^{3+}) ferrite

synthesized by co-precipitation method with ultrasonic irradiation, Journal of Magnetism and Magnetic Materials, 460 (2018) 89-94.

28. P.A.Vinosha, B.Xavier, A.Ashwini, L.A.Mely, S.J.Das, Tailoring the Photo-Fenton activity of nickel ferrite nanoparticles synthesized by low-temperature co-precipitation technique, Optik, 137 (2017) 2442-2453.

29. A.Nadumane, K.Shetty, K.S.Anantharaju, H.P.Nagaswarupa, D.Rangappa, Y.S.Vidhya, H.Nagabhushana, S.C.Prashantha, Sunlight photocatalytic performance of Mg doped nickel ferrite synthesized by a green sol-gel route, Journal of Science; Advanced Materials and Devices, 4 (2019) 89-100.

30. P.Chand, S.Vaish, P.Kumar, Structural, optical and dielectric properties of transition metal (MFe_2O_4; M=Co,Ni and Zn) nanoferrites, Physica B: Condensed Matter, 524 (2017)53-63.

31. N.A.S.Nogueira, V.H.S.Utuni, Y.C.Silva, P.K.Kiyohara, I.F.Vasconcelos, M.A.R.Miranda, J.M.Sasaki, X-ray diffraction and Mossbauer studies on Superparamagnetic nickel ferrite ($NiFe_2O_4$) obtained by the proteic sol-gel method. Materials Chemistry and Physics, 163, 403-406, 2015.

32. M.Venkadesh, G.S.Kumar, S.Viji, S.Karthi, E.K.Girija, Microwave assisted combustion synthesis and characterization of Nickel Ferrite Nanoplatelets, Modern Electronic Materials, 2 (2016) 74-78.

33. R.Rameshbabu, R.Ramesh, S.Kanagesan, A.Karthigeyan, S.Ponnusamy, Synthesis of Superparamagnetic $ZnFe_2O_4$ nanoparticles by surfactant assisted hydrothermal method, Journal of Material Science Materials in Electronics, 24 (2013) 4279-4283.

34. G. Liu G, X.S. Gao, K.F. Wang, D.Y. He, J.P. Li (2016) uniformly mesoporous NiO/$NiFe_2O_4$ biphasic nanorods as efficient oxygen evolving catalyst for water splitting.Int J Hydrog Energy 41:17976–17986.

35. K.Panwar, S. Tiwari, K. Bapna, N.L.Heda, R.J. Choudhary, D.M. Phase, B.L. Ahuja (2017) The effect of Cr substitution on the structural, electronic and magnetic properties of pulsed laser deposited NiFe2O4 thin films. J MagnMagn Mater 421:25–30.

36. M. Hua, L. Xu, F. Cui, J. Lian, Y. Huang, J. Bao, J. Qiu, Y. Xu, H. Xu, Y. Zhao, H. Li, Hexamethylenetetramine-assisted hydrothermal synthesis of octahedral nickel ferrite oxide nanocrystallines with excellent supercapacitive performance. J Mater Sci (2018) 53:7621–7636.

37. Liu Y, Li J, Li F, Li W, Yang H, Zhang X, Liu Y, Ma J (2016) A facile preparation of $CoFe_2O_4$ nanoparticles on polyaniline-functionalized carbon nanotubes as enhanced catalysts for the oxygen evolution reaction. J Mater Chem A 4:4472–4478.

38. Huhu Yue, Wanli Zhang, Bo Yu, Yang Hu, Yingjiong Lu, Yuanfu Chen, and Dongxu Yang, Three-dimensional porous cobalt ferrite and carbon nanorod hybrid network as highly efficient electrocatalyst for oxygen evolution reaction, Journal of Material Science, (2020) 55, 11489-11500.

39. Li T, Lv Y, Su J, Wang Y, Yang Q, Zhang Y, Zhou J, Xu L, Sun D, Tang Y (2017) Anchoring $CoFe_2O_4$ nanoparticles on N-doped carbon nanofibers for high-performance oxygen evolution reaction. AdvSci 4:1700226.

40. K.Ishaq, A.A.Saka, A.O.Kamardeen, A.Ahamed, Characterization and antibacterial activity of nickel ferrite doped α-alumina nanoparticle, Engineering science and technology, an international journal, 20 (2) 2017, 563-569.